Proc. Natl. Acad. Sci. USA
Vol. 89, pp. 11814–11817, December 1992
Biochemistry

Characterization of the Ca^{2+}-triggered conformational transition in troponin C

(muscle contraction/calcium regulation/resonance energy transfer)

ZHIYAN WANG*, JOHN GERGELY*†‡, AND TERENCE TAO*§¶

*Department of Muscle Research, Boston Biomedical Research Institute, 20 Staniford Street, Boston, MA 02114; †Neurology Service, Massachusetts General Hospital, Boston, MA 02114; ‡Department of Biological Chemistry and Molecular Pharmacology, Harvard Medical School, Boston, MA 02115; and §Department of Neurology, Harvard Medical School, Boston, MA 02115

Communicated by Manuel F. Morales, September 9, 1992

ABSTRACT **Troponin C is the Ca^{2+}-binding subunit of troponin in vertebrate striated muscle. Binding of Ca^{2+} to troponin C is thought to induce a conformational change that triggers subsequent events in the initiation of muscle contraction. A molecular modeling study has proposed that, when Ca^{2+} binds to the N-terminal triggering sites, helices B and C separate from the helices D and A, thereby exposing a crucial interaction site for troponin I, the inhibitory subunit of troponin [Herzberg, O., Moult, J., and James, M. N. G. (1986) *J. Biol. Chem.* 261, 2638–2644]. In the present study the question of whether this separation actually occurs is addressed directly. A mutant rabbit skeletal troponin C containing a pair of cysteines at position 12 in helix A and position 49 in the polypeptide segment linking helices B and C was created by site-directed mutagenesis. Pyrene excimer fluorescence and resonance energy transfer studies on the labeled mutant troponin C reveal a Ca^{2+}-induced increase in distance between the two cysteines. Under certain assumptions, the distance increase could be estimated from the extent of energy transfer to be ≈13 Å, in good agreement with the distance increase predicted by molecular modeling. Our results provide further experimental support for the model proposed by Herzberg *et al.* (above).**

Contraction of vertebrate striated muscle is regulated by Ca^{2+} and requires the regulatory proteins troponin and tropomyosin (1). Troponin is composed of three subunits, the Ca^{2+}-binding (TnC), inhibitory (TnI), and tropomyosin-binding (TnT) subunits. The crystal structure of TnC reveals a dumbbell-shaped structure, with the N- and C-terminal domains well separated by a central linking helix (2, 3). Binding of Ca^{2+} to the low-affinity triggering sites (sites I and II) in the N-terminal domain of TnC is thought to induce a conformational change in TnC, whereupon changes in the interactions between TnC and TnI, TnI and actin, tropomyosin and actin, and myosin crossbridges and actin occur in succession (4). The nature of this Ca^{2+}-induced conformational change in TnC has been a subject of long-standing interest. By comparing the atomic structures of the Ca^{2+}-free N-terminal domain to that of the Ca^{2+}-bound C-terminal domain, Herzberg *et al.* (5) proposed that binding of Ca^{2+} to the triggering sites induces a movement of helices B and C (helices in TnC are designated by letters according to ref. 2) away from helices A and D, thereby exposing a putative TnI interaction site. Results from recent site-directed mutagenesis studies (6–8) are consistent with this hypothesis but do not directly demonstrate the occurrence of the movement.

For the present study, we constructed a mutant rabbit skeletal TnC (designated as $TnC^{12/49}$) in which Ser-12 and Thr-49 in the N-terminal domain were converted to cysteines by *in vitro* mutagenesis. Pyrene (Pyr) excimer emission and resonance energy transfer (RET) measurements were then carried out to examine whether the distance between probes attached at the inserted cysteines is Ca^{2+}-dependent. The choice of these two particular positions is governed by two major considerations. (*i*) The atomic structure of TnC shows that the side chains at both positions are not engaged in any intramolecular interactions, are exposed to solvent, and point away from the interior of the protein. This minimizes the possibility that the mutations cause disruption of the protein folding, increases the likelihood that the cysteines are fairly reactive, and ensures that probes attached at these cysteines are relatively mobile. (*ii*) The two positions are so located that the model of Herzberg *et al.* (5) predicts a change in distance of ≈11 Å, a sufficiently large change that can readily be detected by the above distance-sensitive spectroscopic methods.

EXPERIMENTAL PROCEDURES

$TnC^{12/49}$ cDNA was constructed from wild-type rabbit skeletal TnC cDNA (9) by first mutating the TGC codon of Cys-98 to the CTT codon of leucine. The AGC and ACA codons of Ser-12 and Thr-49, respectively, were then simultaneously mutated to the TGC codon of cysteine. Mutagenesis, bacterial over-expression, and purification followed methods as described (8).

Pyr-labeled $TnC^{12/49}$ (Pyr-$TnC^{12/49}$) was prepared by incubating $TnC^{12/49}$ with *N*-(1-pyrene)maleimide (Molecular Probes) at a probe/protein molar ratio of 20:1 in a medium containing 5 M guanidinium chloride, 2 mM EDTA, and 20 mM Hepes (pH 7.5) for 6 hr at room temperature and then overnight at 4°C. After quenching the reaction with excess dithiothreitol, the mixture was dialyzed against the reaction medium and then against 0.1 M NaCl/0.1 M Tris·HCl, pH 9.0, to convert the attached Pyr moiety from type I to type II (10). The sample was finally dialyzed against 0.1 M NaCl/0.1 mM $CaCl_2$/20 mM Hepes, pH 7.5, prior to measurements. The measured labeling ratio was 2.0 mol of Pyr per mol of $TnC^{12/49}$ by using $\varepsilon_{343} = 2.3 \times 10^4\ M^{-1}\cdot cm^{-1}$ for the Pyr moiety (10) and the Bradford method for measuring protein concentrations. The error in labeling ratios was estimated to be ≈10%.

Dansyl (DAN)-labeled $TnC^{12/49}$ (DAN-$TnC^{12/49}$) was prepared by incubating $TnC^{12/49}$ with *N*-iodoacetyl-*N'*-(5-sulfo-1-naphthyl)ethylenediamine (1,5-IAEDANS) (Aldrich) at a probe/protein molar ratio of 0.5:1 in a medium containing 0.1 M NaCl, 0.1 mM $CaCl_2$, and 20 mM Hepes (pH 7.5). The reaction was allowed to proceed at room temperature with gentle shaking for 4 hr. Excess dithiothreitol was added to

The publication costs of this article were defrayed in part by page charge payment. This article must therefore be hereby marked "*advertisement*" in accordance with 18 U.S.C. §1734 solely to indicate this fact.

Abbreviations: TnC, TnI, and TnT, the Ca^{2+}-binding, inhibitory, and tropomyosin-binding subunits of troponin, respectively; 1,5-IAEDANS, *N*-iodoacetyl-*N'*-(5-sulfo-1-naphthyl)ethylenediamine; DAN, dansyl; DDP, *N*-(4-dimethylamino-3,5-dinitrophenyl); Pyr, pyrene; RET, resonance energy transfer.

¶To whom reprint requests should be addressed at *.

quench the reaction and followed by dialysis against the reaction medium. $TnC^{12/49}$ labeled with both the DAN and the *N*-(4-methylamino-3,5-dinitrophenyl) (DDP) moieties (DAN-DDP-$TnC^{12/49}$) was prepared by incubating DAN-$TnC^{12/49}$ with *N*-(4-dimethylamino-3,5-dinitrophenyl)maleimide (Aldrich) at a probe/protein ratio of 5:1 in the above reaction medium for 5 hr at room temperature and then overnight at 4°C. The reaction was quenched and dialyzed against reaction medium. Measured molar labeling ratios for DAN-DDP-$TnC^{12/49}$ were 0.4:1.5:1.0 (DAN/DDP/$TnC^{12/49}$), by using $\varepsilon_{337} = 6000\ M^{-1}\cdot cm^{-1}$ for the DAN moiety (11) and $\varepsilon_{442} = 2930\ M^{-1}\cdot cm^{-1}$ for the DDP moiety (12).

Pyr emission spectra were recorded on a SPEX Fluorolog 2 spectrofluorimeter. Fluorescence decay curves were recorded on a modified ORTEC 9200 nanosecond fluorometer and analyzed by the method of moments (13). The activities of unlabeled and labeled $TnC^{12/49}$ in myofibrils were assayed as in ref. 6.

RESULTS AND DISCUSSION

The emission spectrum of Pyr-$TnC^{12/49}$ (Fig. 1*A*) was recorded under the following three metal binding conditions: (*i*) the apo state in which none of the metal binding sites are occupied; (*ii*) the Mg^{2+} state in which the high-affinity sites (III and IV) are occupied by Mg^{2+}, simulating the *in vivo* relaxed state; and (*iii*) the Ca^{2+} state in which both the high- and the low-affinity triggering sites (I and II) are occupied by Ca^{2+}, simulating the *in vivo* contracting state. Whereas the emission <450 nm is characteristic of Pyr monomers, the broad band >450 nm arises from excited state dimers (excimers) formed when the two pyrene moieties are sufficiently close to each other (14, 15). The results show that the intensity of the excimer band is relatively unaffected by the occupancy of the high-affinity sites by Mg^{2+} but decreases significantly when the low-affinity sites are occupied by Ca^{2+}. This suggests that, in the two Ca^{2+}-free states (apo and Mg^{2+} states), the Pyr moieties are sufficiently close to each other to form some excimers, but, upon binding of Ca^{2+} to the low-affinity sites, the two cysteines and the Pyr moieties move away from each other so that the probability for excimer formation is decreased. The same results were obtained when Pyr-$TnC^{12/49}$ was complexed with TnI (Fig. 1*B*) or with both TnI and TnT (Fig. 1*C*), indicating that TnI and TnT do not affect the Ca^{2+}-induced distance increase.

The fluorescence decay of DAN-$TnC^{12/49}$ in the Ca^{2+} state was found to be adequately described by a single exponential with a lifetime of 13.3 ns (Fig. 2*A* and Table 1). Independent measurements of DAN-TnC^{12} and DAN-TnC^{49} (1,5-IAEDANS-labeled TnC mutants with single cysteines at positions 12 and 49, respectively) yielded monoexponential fluorescence decays with lifetimes of 13.9 and 13.8 ns, respectively (T.T., unpublished results). Evidently the environments around Cys-12 and Cys-49 are nearly identical so that even though both cysteines in $TnC^{12/49}$ can be expected to be labeled by 1,5-IAEDANS, only one lifetime is manifested in the fluorescence decay of DAN-$TnC^{12/49}$. The fluorescence lifetime of DAN-$TnC^{12/49}$ is the same in the three metal binding states that we studied (Table 1). When complexed with either TnI or with both TnI and TnT, the lifetime of DAN-$TnC^{12/49}$ increases to ≈16 ns and is again the same irrespective of metal binding state (Table 1).

The fluorescence decay of DAN-DDP-$TnC^{12/49}$ is markedly Ca^{2+}-dependent; compared to the decay of DAN-$TnC^{12/49}$, it is considerably quenched in the apo and Mg^{2+} states and only slightly quenched in the Ca^{2+} state (Fig. 2), indicating that considerably more energy transfer takes place in the Ca^{2+}-free states than in the Ca^{2+}-saturated state. In conjunction with the Pyr-excimer results, these observations provide

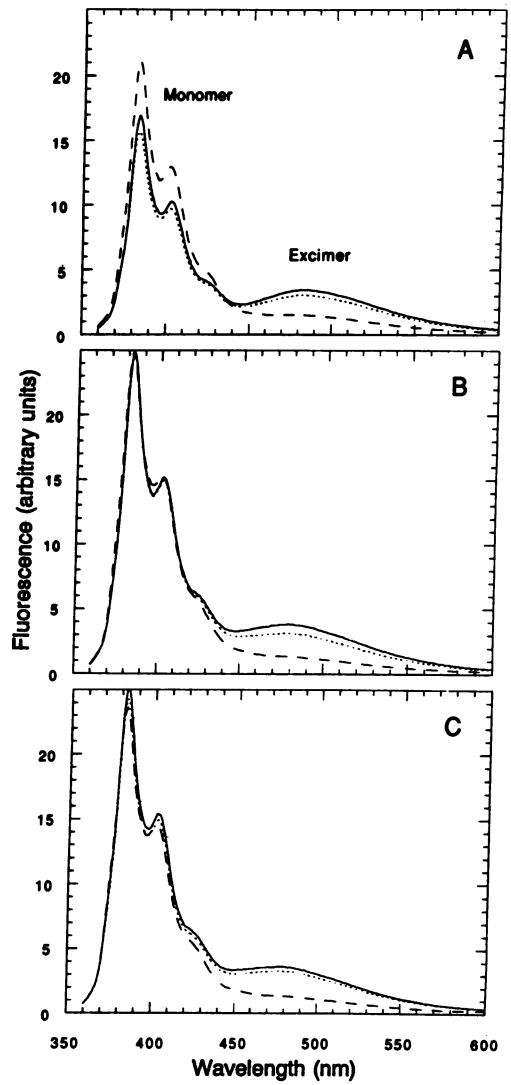

FIG. 1. Emission spectra of Pyr-$TnC^{12/49}$ in the uncomplexed state (*A*), complexed with TnI (*B*), and complexed with both TnI and TnT (*C*). Spectra were taken using the same sample with 0.1 mM $CaCl_2$ for the Ca^{2+} state (dashed line); 0.1 mM $CaCl_2$ and 2 mM EGTA for the apo state (solid line); and 0.1 mM $CaCl_2$, 2 mM EGTA, and 4 mM $MgCl_2$ for the Mg^{2+} state (dotted line). The sample was contained in 20 mM Hepes/0.1 M NaCl (pH 7.5) at a protein concentration of 2.5 μM and a temperature of 25°C. The excitation wavelength was 345 nm.

qualitative evidence for an increase in the distance between the probes when Ca^{2+} binds to the triggering sites.

An attempt was made to estimate the actual distance change from the fluorescence decay data. The DAN-DDP-$TnC^{12/49}$ decay curves were subjected to method-of-moments analyses. The results show that, for the Mg^{2+} state, two lifetimes describe the decay adequately (Fig. 1*B*). When triexponential analysis was carried out, a third lifetime of negligible amplitude was obtained. Of the two lifetimes, one (13.4 ns) is nearly identical to that of DAN-$TnC^{12/49}$ (13.3 ns), while the second (5.6 ns) is considerably shorter (Table 1).

These observations can be interpreted as follows. The DAN-DDP-$TnC^{12/49}$ preparation is composed of a statistical mixture of the following four species: (*i*) $TnC^{12/49}$ with both cysteines labeled with DDP, (*ii*) $TnC^{12/49}$ with both cysteines labeled with DAN, (*iii*) $TnC^{12/49}$ with Cys-12 labeled with DAN and Cys-49 labeled with DDP, and (*iv*) $TnC^{12/49}$ with Cys-12 labeled with DDP and Cys-49 labeled with DAN. The first species is not detected by the fluorescence lifetime

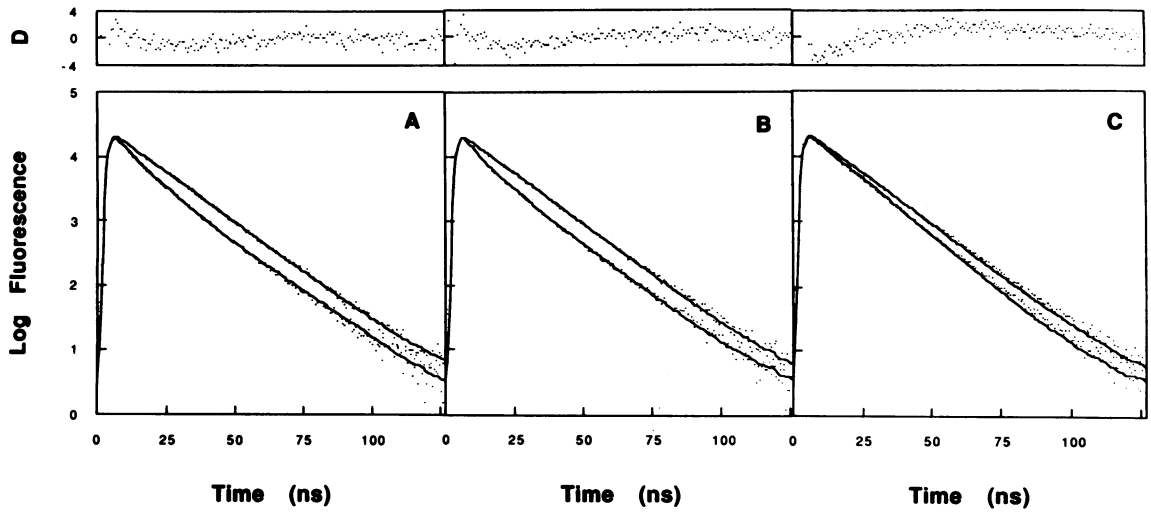

FIG. 2. Fluorescence decay curves of DAN-TnC$^{12/49}$ (upper curves) and DAN-DDP-TnC$^{12/49}$ (lower curves) in the apo (*A*), Mg^{2+} (*B*), and Ca^{2+} (*C*) states. Dots are experimental points, solid lines are calculated curves using parameters derived from method-of-moments analyses (Table 1). Upper panels show the weighted deviation function *D* for the DAN-DDP-TnC$^{12/49}$ curves. $D = (c_i - e_i)/(e_i)^{1/2}$, where e_i and c_i are the *i*th experimental and calculated values, respectively. Excitation and emission were selected by Corning CS7-51 and CS3-69 glass filters, respectively. Other conditions were identical to those specified in Fig. 1.

measurement since the DDP acceptor is nonfluorescent. The fluorescence decay of the second species is identical to that of DAN-TnC$^{12/49}$. If there is donor-to-acceptor energy transfer, the last two species would have the same lifetime, but one that is shorter than that of DAN-TnC$^{12/49}$ due to quenching of donor fluorescence decay by the Förster mechanism. The composite is the observed biexponential decay with one lifetime that is identical to that of DAN-TnC$^{12/49}$ and a second one that is shorter than that of DAN-TnC$^{12/49}$.

The transfer efficiency and the donor–acceptor separation distance were obtained from the Förster equations (Table 1) by taking the lifetime of DAN-TnC$^{12/49}$ as τ_d and the shorter lifetime of DAN-DDP-TnC$^{12/49}$ as τ_{da} and assuming that the orientation factor κ^2 takes on the isotropically averaged value of 2/3. The results (Table 1) show that in the Mg^{2+} state the transfer efficiency is relative high and corresponds to a relatively short interprobe distance of 26 Å. Measurements made in the apo state yielded a similar distance of 28 Å.

For DAN-DDP-TnC$^{12/49}$ in the Ca^{2+} state, the extent of quenching is so small that only a single exponential with a lifetime of 12.0 ns was detectable. Taking this lifetime as an approximation of τ_{da}, a distance of 39 Å was obtained. We conclude that, when Ca^{2+} binds to the low-affinity sites, the distance between probes attached at residues 12 and 49 in TnC increases by ≈13 Å.

Measurements were also made in the presence of TnI and of both TnI and TnT. We found that τ_d and τ_{da} increase upon the binding of TnI or of TnI and TnT (Table 1), but the

Table 1. Fluorescence decay and energy transfer parameters

Sample	A_1	τ_1, ns	A_2	τ_2, ns	$\chi^2/(N-p)$	E	R_0, Å	R, Å
DAN-TnC$^{12/49}$, uncomplexed, Ca^{2+}	1.00	13.3	—	—	2.4			
DAN-DDP-TnC$^{12/49}$, uncomplexed, Ca^{2+}	1.00	12.0	—	—	2.6	0.10	27	39
DAN-TnC$^{12/49}$, uncomplexed, Mg^{2+}	1.00	13.4	—	—	1.5			
DAN-DDP-TnC$^{12/49}$, uncomplexed, Mg^{2+}	0.58	5.6	0.42	13.4	2.5	0.58	27	26
DAN-TnC$^{12/49}$, uncomplexed, apo	1.00	13.5	—	—	1.3			
DAN-DDP-TnC$^{12/49}$, uncomplexed, apo	0.73	7.3	0.27	15.2	2.5	0.46	27	28
DAN-TnC$^{12/49}$ + TnI, Ca^{2+}	1.00	15.6	—	—	2.1			
DAN-DDP-TnC$^{12/49}$ + TnI, Ca^{2+}	1.00	14.3	—	—	2.2	0.08	28	41
DAN-TnC$^{12/49}$ + TnI, Mg^{2+}	1.00	16.3	—	—	3.1			
DAN-DDP-TnC$^{12/49}$ + TnI, Mg^{2+}	0.74	9.3	0.26	19.0	2.5	0.43	28	29
DAN-TnC$^{12/49}$ + TnI, apo	1.00	16.5	—	—	2.5			
DAN-DDP-TnC$^{12/49}$ + TnI, apo	0.68	9.3	0.32	18.2	2.0	0.44	28	29
DAN-TnC$^{12/49}$ + TnI + TnT, Ca^{2+}	1.00	16.2	—	—	2.4			
DAN-DDP-TnC$^{12/49}$ + TnI + TnT, Ca^{2+}	1.00	14.3	—	—	3.4	0.12	28	39
DAN-TnC$^{12/49}$ + TnI + TnT, Mg^{2+}	1.00	17.2	—	—	2.7			
DAN-DDP-TnC$^{12/49}$ + TnI + TnT, Mg^{2+}	0.73	9.4	0.27	18.8	3.0	0.45	28	29
DAN-TnC$^{12/49}$ + TnI + TnT, apo	1.00	17.2	—	—	2.7			
DAN-DDP-TnC$^{12/49}$ + TnI + TnT, apo	0.67	8.5	0.33	18.2	1.6	0.51	28	28

A_1, A_2, are fractional amplitudes and τ_1, τ_2 are lifetimes derived from method-of-moments analysis. Experimental uncertainty in τ was estimated to be 0.1 ns for monoexponential lifetimes and 0.6 ns for biexponential lifetimes. $\chi^2/(N-p)$ is the mean squared residue, where $\chi^2 = \Sigma_{i=1}^{N} (c_i - e_i)^2/e_i$, c_i and e_i are the *i*th calculated and experimental values, respectively, N is the number of time points, and p is the number of decay parameters. For all the decay curves, the addition of another exponential in the analysis yielded a negligible amplitude and only small changes in the other parameters. E is the transfer efficiency, defined as $E = (1 - \tau_{da}/\tau_d)$, where τ_d and τ_{da} are donor fluorescence lifetimes in the absence and presence of acceptor, here taken as τ_1 of DAN-TnC$^{12/49}$ and DAN-DDP-TnC$^{12/49}$, respectively (see text for justification). R_0 is the critical transfer distance assuming the orientation factor κ^2 to be 2/3. R_0 for the DAN–DDP couple was reported to be 29 Å, with a donor fluorescence lifetime of 20.6 ns (12). For this work we corrected for the variation of R_0 with donor fluorescence quantum yield using the equation $R_0 = R_0' (\tau_d/\tau_d')^{1/6}$, where $R_0' = 29$ Å and $\tau_d' = 20.6$ ns. R is the separation distance, calculated from the equation $R = R_0(E^{-1} - 1)^{1/6}$.

calculated transfer efficiencies and separation distances are similar to those for uncomplexed $TnC^{12/49}$; the Ca^{2+}-induced distance change of 10–12 Å also appears to be unaffected by TnI and TnT, in agreement with the Pyr excimer results.

In an approximate assessment of the validity of our assumption that κ^2 takes on the isotropic value of 2/3, the limiting emission anisotropy A_0 of DAN-$TnC^{12/49}$ in the Ca^{2+} state was measured by extrapolation of the anisotropy decay curve (data not shown) to zero time. A value of 0.17 was obtained. For comparison A_0 values for DAN-TnC^{12} and DAN-TnC^{49} are both 0.18 (T.T., unpublished results). These A_0 values are considerably smaller than the theoretical maximum of 0.4, indicating that the orientation of the donor's transition moment is somewhat randomized within the probe's excited state lifetime. By using equations in Stryer (16), the uncertainty in the calculated distance was estimated to be 32% when only randomization of the donor transition moment was taken into account. Since both probe attachment sites were chosen to have exposed environments, the acceptor is likely to have some flexibility, so that this uncertainty can be expected to be smaller when randomization of the acceptor orientation was taken into account. This, however, could not be assessed directly since the DDP moiety is not fluorescent.

Values of A_0 for DAN-$TnC^{12/49}$ in the apo and Mg^{2+} states were measured to be 0.18 and 0.19, respectively, similar to that in the Ca^{2+} state. This indicates that the degree of probe transition moment randomization is independent of metal ion occupancy state, so that our observed changes in the energy transfer efficiency and the calculated distance are not likely to be due to changes in the magnitude of κ^2.

We found that unlabeled $TnC^{12/49}$ and all the labeled $TnC^{12/49}$ molecules were capable of regulating myofibrillar ATPase activity in a Ca^{2+}-dependent manner (Fig. 3), indicating that neither the mutations nor the labeling have any major deleterious effects on the activity of TnC.

The distances obtained here may be compared with those obtained by crystallography and molecular modeling. The crystallographic atomic structure of TnC with only the high-affinity sites occupied by Ca^{2+} shows that the distance between the α-carbons of residues 12 and 49 is 21 Å (2, 3), while our RET-derived interprobe distance for TnC12/49 in the Mg^{2+} state is 26 Å. The agreement is reasonable and lends confidence to the assumptions that were made to obtain the distance information. That the RET-derived distance is somewhat larger may be attributed to the fact that the probes have finite sizes and are attached two atoms away from the α-carbons. By molecular modeling, Herzberg *et al.* (5) derived an atomic structure of Ca^{2+}-saturated TnC in which the distance between the α-carbons of residues 12 and 49 would be 32 Å, and our RET-derived interprobe distance for $TnC^{12/49}$ in the Ca^{2+} state is 39 Å. The Ca^{2+}-induced increase in distance predicted by molecular modeling is, therefore, 11 Å compared with 13 Å obtained by RET. Again, the agreement is reasonable, and the somewhat larger RET-derived values may reflect the finite sizes of the probes. It should be emphasized that the RET-derived distances were obtained under the assumption that κ^2 takes on the value of 2/3 and that as long as κ^2 cannot be measured directly, the absolute magnitude of our RET-derived distances is not unequivocal. Semiquantitatively, however, we can be reasonably confident that the RET-derived change in distance is comparable to that predicted by the molecular modeling work of Herzberg *et al.* (5).

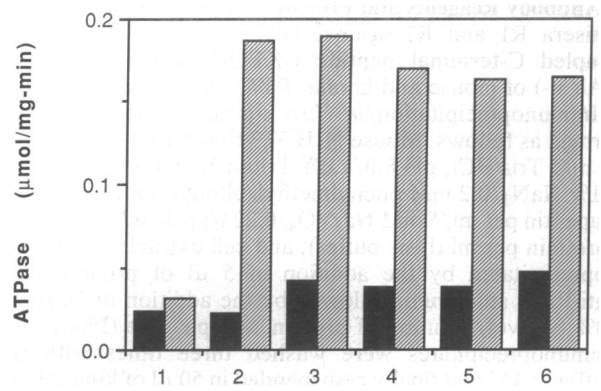

FIG. 3. Ca^{2+}-dependent ATPase activities of TnC-depleted rabbit skeletal myofibrils to which various TnC molecules were readded. Solid and hatched bars are in the absence and presence of Ca^{2+}, respectively. Additions were as follows: Bars: 1, none; 2, TnC purified from rabbit skeletal muscle; 3, $TnC^{12/49}$; 4, DAN-$TnC^{12/49}$; 5, DAN-DDP-$TnC^{12/49}$; 6, Pyr-$TnC^{12/49}$.

In conclusion the results reported here provide further experimental support for the hypothesis of Herzberg *et al.* (5) that Ca^{2+} induces a movement of helices B and C away from helices D and A in the N-terminal domain of TnC. Fujimori *et al.* (7) have found that a genetically engineered salt bridge that can be expected to inhibit partially the occurrence of this Ca^{2+}-induced movement reduced the Ca^{2+} affinity of the triggering sites, a finding that is consistent with the hypothesis. Grabarek *et al.* (6) have shown that a genetically engineered disulfide bond that can be expected to inhibit totally the proposed movement abolished the activity of TnC. Thus, all the current findings indicate that the Ca^{2+}-induced conformational transition proposed by Herzberg *et al.* (5) does occur and that this conformational transition is essential for the regulatory function of TnC.

We are grateful to Dr. Zenon Grabarek for helpful discussions. The work was supported by grants from the National Institutes of Health (AR21673 to T.T. and HL5949 to J.G.) and the Muscular Dystrophy Association (to J.G.).

1. Ebashi, S. & Endo, M. (1968) *Prog. Biophys. Mol. Biol.* **18,** 123–183.
2. Herzberg, O. & James, M. N. G. (1985) *Nature (London)* **313,** 653–659.
3. Sundaralingam, M., Bergstrom, R., Strasburg, G., Rao, S. T., Roychowdhury, P., Greaser, M. & Wang, B. C. (1985) *Science* **227,** 945–948.
4. El-Saleh, S., Warber, K. D. & Potter, J. D. (1986) *J. Muscle Res. Cell Motil.* **7,** 387–404.
5. Herzberg, O., Moult, J. & James, M. N. G. (1986) *J. Biol. Chem.* **261,** 2638–2644.
6. Grabarek, Z., Tan, R.-Y., Wang, J., Tao, T. & Gergely, J. (1990) *Nature (London)* **345,** 132–135.
7. Fujimori, K., Sorenson, M., Herzberg, O., Moult, J. & Reinach, F. C. (1990) *Nature (London)* **345,** 182–184.
8. Wang, Z., Sarkar, S., Gergely, J. & Tao, T. (1990) *J. Biol. Chem.* **265,** 4953–4957.
9. Chen, Q., Taljanidisz, J., Sarkar, S., Tao, T. & Gergely, J. (1988) *FEBS Lett.* **228,** 22–26.
10. Graceffa, P. & Lehrer, S. S. (1980) *J. Biol. Chem.* **255,** 11296–11300.
11. Hudson, E. N. & Weber, G. (1976) *Biochemistry* **15,** 672–680.
12. Dalbey, R. E., Weiel, J. & Yount, R. G. (1983) *Biochemistry* **22,** 4696–4706.
13. Tao, T. & Cho, J. (1979) *Biochemistry* **18,** 2759–2765.
14. Betcher-Lange, S. L. & Lehrer, S. S. (1978) *J. Biol. Chem.* **253,** 3757–3760.
15. Strasburg, G. M., Leavis, P. C. & Gergely, J. (1985) *J. Biol. Chem.* **260,** 366–370.
16. Stryer, L. (1978) *Annu. Rev. Biochem.* **47,** 819–846.